Autonomous Tracking of Salinity-Intrusion Fronts by a Long-Range Autonomous Underwater Vehicle

Yanwu Zhang, *Senior Member, IEEE*, Noa Yoder, Brian Kieft, *Member, IEEE*, Amy Kukulya, Brett W. Hobson, *Member, IEEE*, Svenja Ryan, and Glen G. Gawarkiewicz

***Abstract*—Shoreward intrusions of anomalously salty water along the continental shelf of the Middle Atlantic Bight are often observed in spring and summer. Exchange of heat, nutrients, and carbon across the salinity-intrusion front has a significant impact on the marine ecosystem and fisheries. In this article, we developed a method of using an autonomous underwater vehicle (AUV) to detect a salinity-intrusion front and track the front's movement. Autonomous front detection is based on the different vertical structures of salinity in the two distinct water types: the vertical difference of salinity is large in the intruding saltier water because of the salinity "tongue" at mid-depth, but is small in the nearshore fresher water due to absence of the salinity anomaly. Every time the AUV crosses and detects the front, the vehicle makes a turn at an oblique angle to cross the front, thus zigzagging through the front to map the frontal zone. The AUV's zigzags sweep back and forth to track the front as it moves over time. From June 25 to 30, 2021, a *Tethys*-class long-range AUV mapped and tracked a salinity-intrusion front on the southern New England shelf. The frontal tracking revealed the salinity intrusion's 3-D structure and temporal evolution with unprecedented detail.**

***Index Terms*—Autonomous underwater vehicle (AUV), front, Middle Atlantic Bight, salinity intrusion, southern New England shelf, track.**

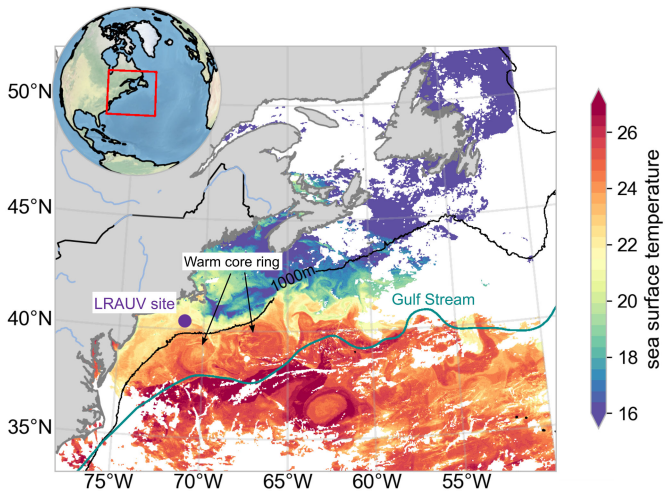

Fig. 1. Snapshot of the advanced very-high-resolution radiometer (AVHRR) sea surface temperature (SST) on June 29, 2021. The mean Gulf Stream path (25-cm sea surface height contour) between 1993 and 2017 [8], two warm core rings, and the long-range AUV (LRAUV) operation site are marked.

I. Introduction

THE Gulf Stream is a western-boundary current that flows poleward and brings warm water from the Gulf of Mexico into the North Atlantic Ocean. Around Cape Hatteras (∼30 °N), the Gulf Stream separates from the coast and transitions into a free flowing current, which starts meandering. As a consequence, warm and salty eddies, called "warm core rings" [1], break off the Gulf Stream and move northwestward through the Slope Sea [2], impinging onto the continental slope and ultimately the continental shelf [see Fig. 1]. Along the continental shelf of the Middle Atlantic Bight (from Georges Bank to Cape Hatteras), shoreward intrusion of anomalously salty water is often observed in spring and summer [1], [3], [4]. Fronts are formed between the relatively fresh shelf water and the intruding saltier water. The cross-frontal exchange of heat, nutrients, and carbon between the continental slope and the continental shelf [1], [5] has a significant impact on marine ecology [6] and fishery [7]. The existence of salinity intrusions has been known for decades but 3-D hydrographic mapping of their structure was rarely made, impeding a deeper understanding of this important process. Their complex structure poses an immense challenge on traditional oceanographic sampling methods and calls for new innovative sampling strategies.

Autonomous platforms have found applications in studies of ocean fronts. A sub-surface neutrally buoyant Lagrangian float was deployed in the Kuroshio front to reveal that ocean fronts enhance energy dissipation in the surface boundary layer [9]. Autonomous underwater vehicles (AUVs) and a Wave Glider were effectively used to map and track coastal upwelling fronts in Monterey Bay by zigzagging across the fronts [10], [11]. The AUV autonomously detected the front based on the different vertical structures of temperature in the two distinct water types [10]. The Wave Glider autonomously detected the front based on the horizontal gradient of the near-surface temperature [11]. In West Antarctica, an AUV surveyed under the Thwaites

Manuscript received September 30, 2021; revised January 14, 2022; accepted January 20, 2022. This work was supported in part by the National Science Foundation under Grant OCE-1851261 and in part by the David and Lucile Packard Foundation. *(Corresponding author: Yanwu Zhang.)*

Associate Editor: B. Englot.

Yanwu Zhang, Brian Kieft, and Brett W. Hobson are with the Monterey Bay Aquarium Research Institute, Moss Landing, CA 95039 USA (e-mail: yzhang@mbari.org; bkieft@mbari.org; hobson@mbari.org).

Noa Yoder, Amy Kukulya, Svenja Ryan, and Glen G. Gawarkiewicz are with the Woods Hole Oceanographic Institution, Woods Hole, MA 02543 USA (e-mail: nyoder@whoi.edu; akukulya@whoi.edu; sryan@whoi.edu; ggawarkiewicz@whoi.edu).

Digital Object Identifier 10.1109/JOE.2022.3146584

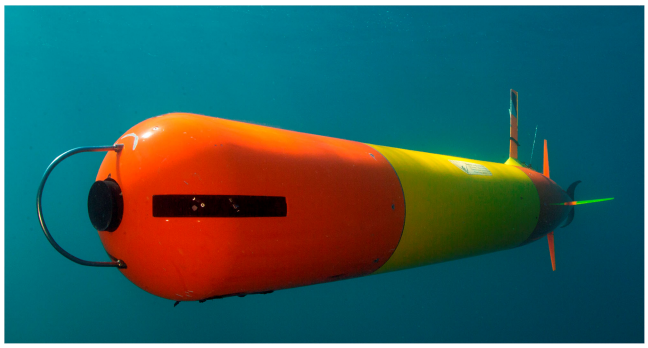

Fig. 2. *Tethys*-class LRAUV (photo courtesy of Kip Evans).

Ice Shelf front where inflow of warmer water and outflow of melt-enriched colder water meet and mix [12]. In the Arctic, an AUV autonomously tracked a front near an ice edge using near-surface averaged temperature as the feature [13]. In the northeast Pacific, an AUV was deployed to track a salinity front by zigzagging between two boundaries defined by a lower- and a higher-salinity bound (at a specific depth) [14]. The salinity bounds were determined based on preceding ship underway surveys and measurements by autonomous surface vehicles.

In this article, we developed a method for an AUV to autonomously detect a salinity-intrusion front and track its movement over time. Front detection is not based on absolute levels of salinity, but on the different vertical structures of salinity in the two distinct water types. *Tethys*-class LRAUVs are described in Section II. The algorithms are presented in Section III. In June 2021, LRAUV *Polaris* mapped and tracked a salinity-intrusion front on the southern New England shelf, as reported in Section IV. Conclusions and future work are discussed in Section V.

II. *Tethys*-Class LRAUV

A *Tethys*-class LRAUV [see Fig. 2] is 2.3–3.2 m long (depending on the payload configuration), and has a diameter of 0.3 m at the midsection. It can run from 0.5 to 1 m/s using a propeller. Using a primary battery, the vehicle has demonstrated a range of 1800 km (three-week duration) at 1-m/s speed [15]. Long range is realized by minimizing propulsion power consumption through an innovative design of a low-drag body and a high-efficiency propulsion system [16]. In addition, the vehicle is equipped with a buoyancy engine and is capable of autoballasting to neutral buoyancy, which allows flight at a reduced angle of attack to decrease drag. Using the buoyancy engine, the vehicle is capable of drifting in a lower-power state and controlling depth while the thruster is powered off. An LRAUV thus combines mobility and speed properties typical to propelled vehicles and energy-saving properties unique to buoyancy-driven vehicles. An LRAUV's science sensor suite (all in the nose section) includes Sea-Bird SBE GPCTD temperature, conductivity, and depth sensors, a Sea-Bird SBE 43F dissolved oxygen sensor, a Sea-Bird SeaOWL-UV-A sensor to measure fluorescent dissolved organic matter (excitation wavelength 370 nm and emission wavelength 460 nm), chlorophyll fluorescence (excitation wavelength 470 nm and emission wavelength 690 nm), and backscatter (700-nm wavelength), and a LI-COR LI-192SA PAR (photosynthetically active radiation) sensor. The vehicle's underwater navigation is by dead reckoning aided by a Doppler velocity log (DVL). The DVL provides the earth-referenced velocity of the vehicle when the ocean bottom is within acoustic range. The vehicle's estimated speed is combined with measured heading and attitude and then accumulated to provide the estimated location. The vehicle periodically ascends to the surface for a global positioning system (GPS) fix to correct the accumulated underwater navigation error [15]. The LRAUV software architecture uses state configured layered control [17], which divides the vehicle operation into a group of behaviors assigned with hierarchical levels of priority. The vehicle runs a mission script that invokes appropriate AUV behaviors to achieve a specified goal [15].

III. Algorithms for Salinity-Intrusion Front Detection and Tracking

A. Front-Detection Algorithm

In the Middle Atlantic Bight during the stratified season, the salinity intrusions often take the form of "tongues" of anomalously salty water with a thickness of about 10 m and centered between 10- and 40-m depths, with a horizontal extent of about 10 km [3]. Our salinity-intrusion front detection algorithm is based on the different vertical structures of salinity in the two distinct water types measured on the AUV's sawtooth (i.e., yo-yo) trajectory, as shown in Fig. 3.

We define the vertical salinity homogeneity index (VSHI), as an extension of the previously defined vertical temperature homogeneity index (VTHI) for upwelling front detection [10]. The VSHI (denoted by ΔS_{vert}) is defined as follows:

$$\Delta S_{\mathrm{vert}} = \frac{1}{N}\sum_{i=1}^{N}\left|S_{\mathrm{depth}_i} - \frac{1}{N}\sum_{i=1}^{N} S_{\mathrm{depth}_i}\right| \tag{1}$$

where i is the depth index, and N is the total number of depths participating in the calculation of ΔS_{vert}; S_{depth_i} is the salinity at the ith depth. $1/N\sum_{i=1}^{N} S_{\mathrm{depth}_i}$ is the average salinity of those depths. $1/N\sum_{i=1}^{N}|S_{\mathrm{depth}_i} - 1/N\sum_{i=1}^{N} S_{\mathrm{depth}_i}|$ measures the difference (absolute value) between the salinity at each individual depth and the depth-averaged salinity. The averaged difference ΔS_{vert} (averaged over all participating depths) is a measure of the vertical homogeneity of salinity in the water column. In the intruding saltier water, salinity is high within the salinity "tongue" at mid-depth, but low below and above the "tongue." Because of the large salinity differences at different depths, ΔS_{vert} is large. In the nearshore fresher water, salinity levels are low at all depths (only slightly higher below the pycnocline than above the pycnocline), so ΔS_{vert} is much smaller than that in the intruding saltier water.

Suppose an AUV flies from the salinity intrusion to the fresher water on a yo-yo trajectory. Fig. 3 illustrates the front detection algorithm. On each yo-yo profile (descent or ascent), the AUV records salinity at the participating depths to calculate ΔS_{vert} in real time. When ΔS_{vert} falls below a threshold $\mathrm{thresh}_{\Delta S_{\mathrm{vert}}}$ for

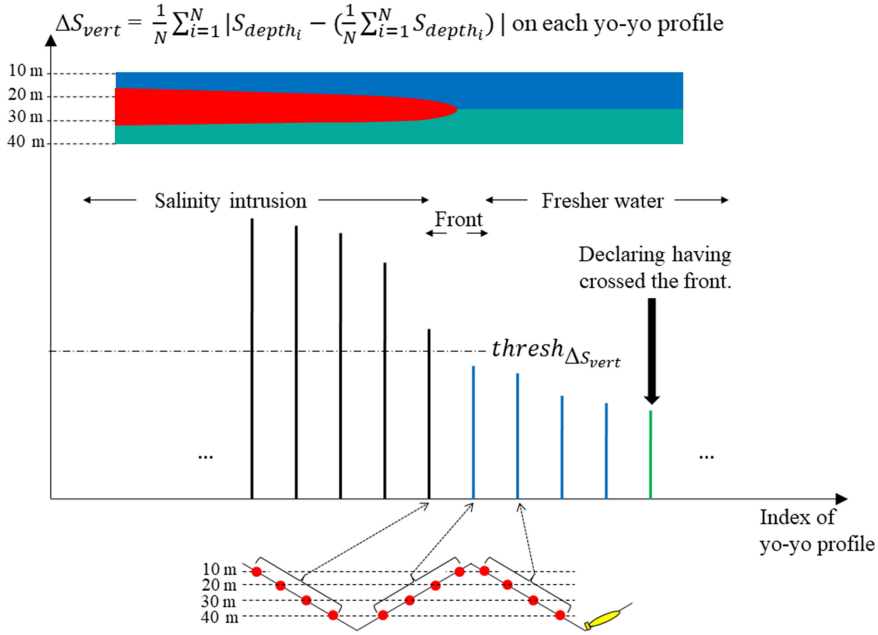

Fig. 3. Illustration of the algorithm for an AUV to determine that it has departed from the salinity intrusion and entered the fresher water. The first four yo-yo profiles that satisfy $\Delta S_{\mathrm{vert}} \leq \mathrm{thresh}_{\Delta S_{\mathrm{vert}}}$ are marked blue. The fifth such yo-yo profile is marked green where the AUV declares that it has crossed the front.

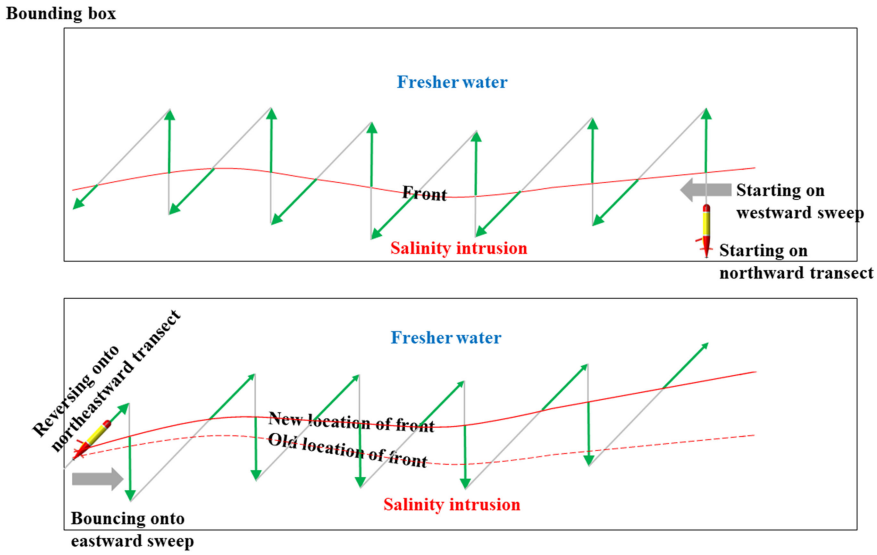

Fig. 4. Illustration of the AUV's horizontal-dimension zigzag tracks alternating in westward and eastward sweeps between a western bound and an eastern bound. Over the duration of the sweeps, the front moved northward. On every instance of front detection, the vehicle continues flight for a prescribed distance (marked green), and then turns an oblique angle to fly back to the other water type. When the AUV reaches the western bound, it reverses course.

a number of consecutive yo-yo profiles, the AUV determines that it has crossed the front and entered the fresher water. Conversely, suppose the AUV flies from the fresher water to the salinity intrusion on a yo-yo trajectory. When ΔS_{vert} rises above $\mathrm{thresh}_{\Delta S_{\mathrm{vert}}}$ for a number of consecutive yo-yo profiles, the AUV determines that it has crossed the front and entered the salinity intrusion. To avoid false detection due to measurement noise or existence of isolated water patches, the algorithm only sets the detection flag when $\mathrm{thresh}_{\Delta S_{\mathrm{vert}}}$ is met on a number of consecutive yo-yo profiles.

B. Front-Tracking Method

Every time the AUV detects the front, it makes a turn at an oblique angle [10]. This way, the vehicle zigzags through the front to map it and track its movement over time. The method is illustrated in Fig. 4, comprising the following steps.

1) The AUV starts from the salinity intrusion (where ΔS_{vert} is high), flying toward the fresher water (where ΔS_{vert} is low), on a yo-yo trajectory between the surface and a depth that is sufficiently deep for manifesting

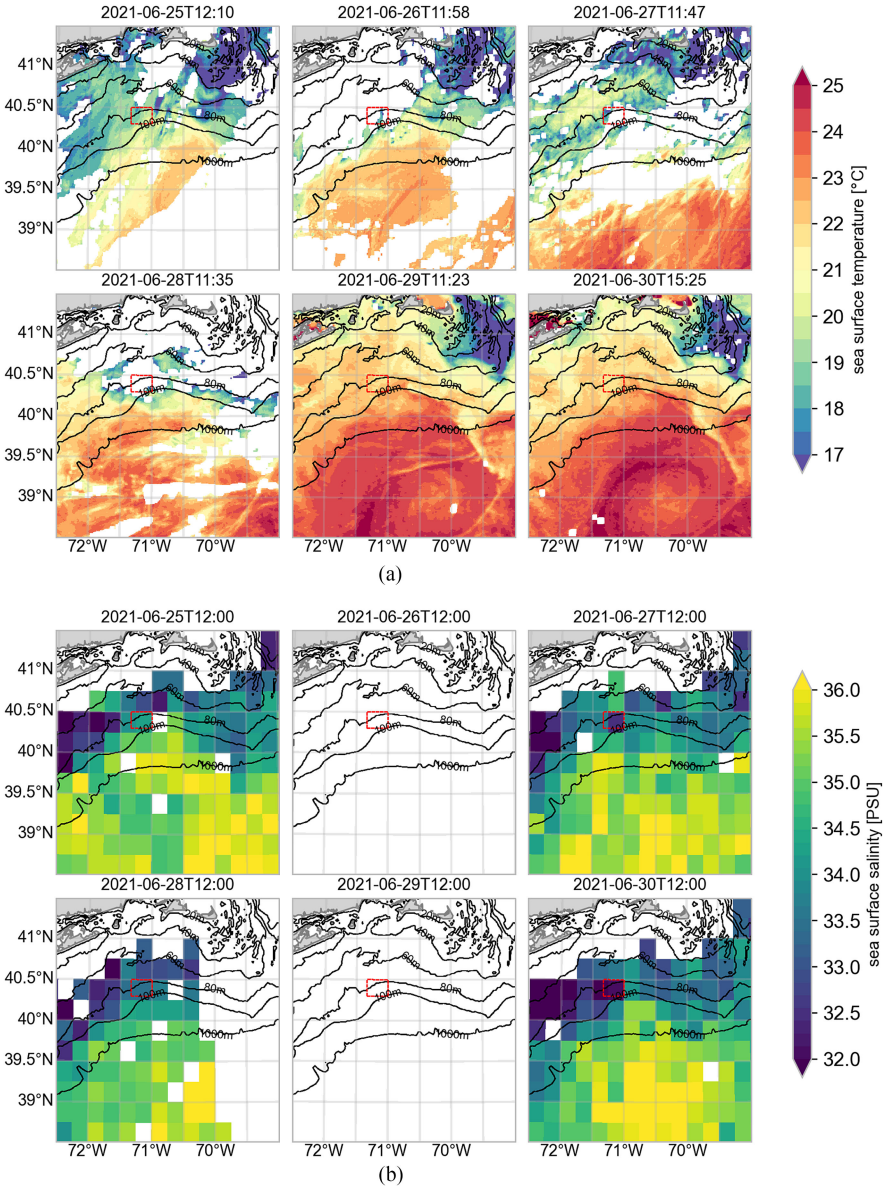

Fig. 5. (a) AVHRR SST images and (b) the Aquarius sea surface salinity (SSS) images of the southern New England shelf and the shelf break between June 25 and 30, 2021. The bounds of the LRAUV salinity-intrusion front-tracking missions are marked by the red dashed line box.

the contrast between the two distinct water types. When ΔS_{vert} falls below $\mathrm{thresh}_{\Delta S_{\mathrm{vert}}}$ for a number of consecutive yo-yo profiles, the AUV determines that it has crossed the front and entered the fresher water.

2) The AUV continues flight in the fresher water for a prescribed distance to sufficiently cover the frontal zone, and then turns an oblique angle to fly back to the salinity intrusion. For the AUV to effectively track the front, the oblique turn angle is set to an appropriate value so that the vehicle intersects the front at a close-to-normal angle (if the AUV's heading is at a small angle to the front or even parallel to it, the vehicle risks losing track of the front).
3) On the way back to the salinity intrusion, when ΔS_{vert} rises above $\mathrm{thresh}_{\Delta S_{\mathrm{vert}}}$ for a number of consecutive yo-yo profiles, the AUV determines that it has crossed the front and entered the salinity intrusion.
4) The AUV continues flight in the salinity intrusion for a prescribed distance, and then turns an oblique angle to fly back to the fresher water.
5) The AUV repeats the aforementioned cycle, thus zigzagging through the frontal zone.
6) The AUV mission terminates once the prescribed mission duration has elapsed.

Front tracking is confined to a bounded region. If the AUV reaches any of the bounds, it turns around to stay inside the bounds. The bounds are defined based on prior information of the front's approximate location and orientation, as well as the AUV operational safety considerations (e.g., away from shore). On a westward-sweeping zigzag (see Fig. 4), when the

AUV reaches the western bound, the vehicle reverses course to start an eastward-sweeping zigzag. Conversely, on an eastward-sweeping zigzag, when the AUV reaches the eastern bound, the vehicle reverses course to start a westward-sweeping zigzag. On each single transect on the zigzag track, if the AUV reaches the northern or southern bound without detecting the front, the vehicle will make a turn onto the next transect that brings the vehicle back into the bounding box.

IV. Experiment

A. Overview

Warmer and saltier water over the continental slope, originating from the Gulf Stream, intrudes shoreward onto the southern New England shelf during summer. In June 2021, *R/V Neil Armstrong* and AUVs were used to investigate salinity intrusions during the Salinity Intrusions, Rings, AUVs, Turbulence, and Squid (SIRATES) experiment. Satellite SST images in the experiment area between June 25 and 30 [see Fig. 5(a)] show how a warm core ring approached the continental shelf. The upper continental slope had anomalously high salinities abutting the fresher shelf water and generated a mid-depth salinity intrusion moving northward onto the shelf. Satellite sea surface salinity (SSS) images [see Fig. 5(b)] show an increasing surface salinity on the continental slope was approaching the shelf, largely consistent with the movement of the warm core ring. However, the satellite measurements were not able to detect subsurface salinity intrusions, which emphasizes the importance of using AUVs to resolve these subsurface intrusions.

Based on the data from an initial cross-shelf shipboard conductivity-temperature-depth transect, we decided to focus on a frontal region marked by the red dashed line box in Fig. 5, and deployed LRAUV *Polaris* to autonomously detect, map, and track the salinity-intrusion front inside the bounding box from June 25 to 30.

B. Parameter Settings

The LRAUV front-tracking parameter settings were based on both historical data and LRAUV measurements. Salinity intrusions over the continental shelf are concentrated at the depth of the seasonal pycnocline [3], [18]. During the stratified season, the intrusions are about 10 m thick and centered between 10- and 40-m depths [3]. LRAUV reconnaissance surveys at the experiment site verified these features. In addition, observations collected from 2015 to 2019 by the commercial fishing industry through the Commercial Fisheries Research Foundation/WHOI Shelf Research Fleet program provided the salinity intrusions' characteristics [19] that allowed fine tuning of the LRAUV front-tracking parameter settings.

1) Participating Depths for Calculating ΔS_{vert}*:* ΔS_{vert} [see (1)] is the key metric used by the LRAUV for classifying the water types (salinity intrusion versus fresher water). We set the participating depths for calculating ΔS_{vert} to 10, 20, 30, and 40 m. To remove anomalous salinity data points, the raw salinity measurements went through a five-point median filter

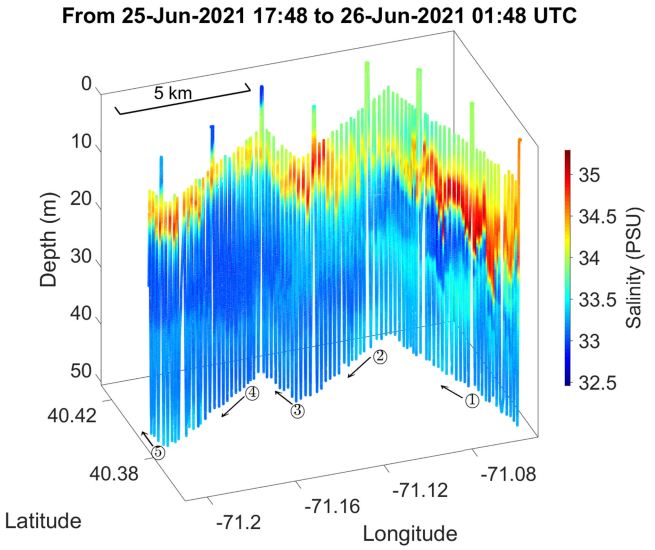

Fig. 6. In one mission on June 25–26, 2021, LRAUV *Polaris* detected and crossed the salinity-intrusion front five times. Front detection on each transect is shown in Fig. 7, with corresponding transect numbers.

(2-s duration corresponding to 0.5-m yo-yo depth change) and then entered the calculation of ΔS_{vert}.

2) Yo-Yo Depth Range: We set the LRAUV yo-yo depth range to 8–50 m. The shallow bound 8 m was for staying clear of boat traffic. The deep bound 50 m was sufficiently deep to depict the salinity-intrusion front. The yo-yo depth range contained all the participating depths for calculating ΔS_{vert}. The vehicle periodically (every hour in the first mission and every 2 h in the succeeding missions) ascended to the surface to obtain GPS fixes and relay decimated science data to shore.

3) Front-Detection Threshold $\mathrm{thresh}_{\Delta S_{\mathrm{vert}}}$ *and Count Requirement:* On each yo-yo profile, the AUV calculates ΔS_{vert} and compares it with a preset threshold $\mathrm{thresh}_{\Delta S_{\mathrm{vert}}}$ to classify the water type. According to the classification theory [20], [21], setting the threshold to the middle level between two classes minimizes the total cost of misclassification. Therefore, we set $\mathrm{thresh}_{\Delta S_{\mathrm{vert}}}$ to the middle of the ΔS_{vert} levels of the two distinct water types. If $\mathrm{thresh}_{\Delta S_{\mathrm{vert}}}$ is set too high or too low, the detected front line will be skewed to one side and the AUV's flight coverage will be excessive in one water type but insufficient in the other. Based on LRAUV surveys prior to the autonomous front-tracking missions, we set $\mathrm{thresh}_{\Delta S_{\mathrm{vert}}}$ to 0.4 PSU for missions from June 25 to 27. Then, we adjusted it to 0.3 PSU for missions from June 27 to 30. To avoid false detection, the algorithm only sets the detection flag when $\mathrm{thresh}_{\Delta S_{\mathrm{vert}}}$ is met on five consecutive yo-yo profiles.

4) Sweep Directions and the Oblique Angle of the Zigzag Track: Preceding surveys indicated that the salinity-intrusion front was oriented east–west. Hence, we let the LRAUV sweep alternately eastward and westward. We set the zigzag oblique turn angle to 135 °, so that the zigzag transects intersected the front at a close-to-normal angle (see Fig. 4). A portion of the eastward sweep from June 27, 23:01 to June 28, 05:34 (UTC) was an exception: the "northeast" direction was set to 60 ° (rather than the routinely set 45 °) to improve the vehicle's eastward

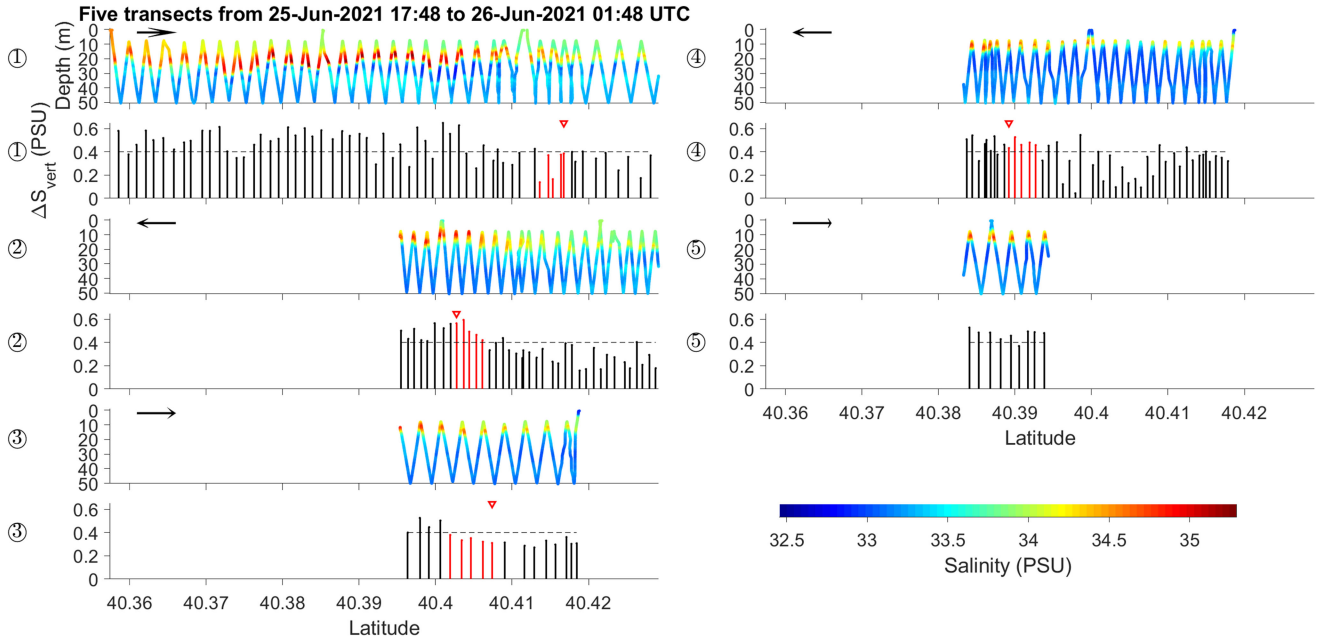

Fig. 7. Salinity and the corresponding ΔS_{vert} on each yo-yo profile in the five cross-front transects shown in Fig. 6. Transect numbers are noted, and each transect has two panels: salinity and ΔS_{vert} on the yo-yo profiles. For each transect, *Polaris*' flight direction is shown by the arrow in the salinity profile panel. The yo-yo profiles that met the $\Delta S_{\mathrm{vert}} \leq \mathrm{thresh}_{\Delta S_{\mathrm{vert}}}$ (if entering the fresher water) or $\Delta S_{\mathrm{vert}} \geq \mathrm{thresh}_{\Delta S_{\mathrm{vert}}}$ (if entering the salinity intrusion) criterion are marked red.

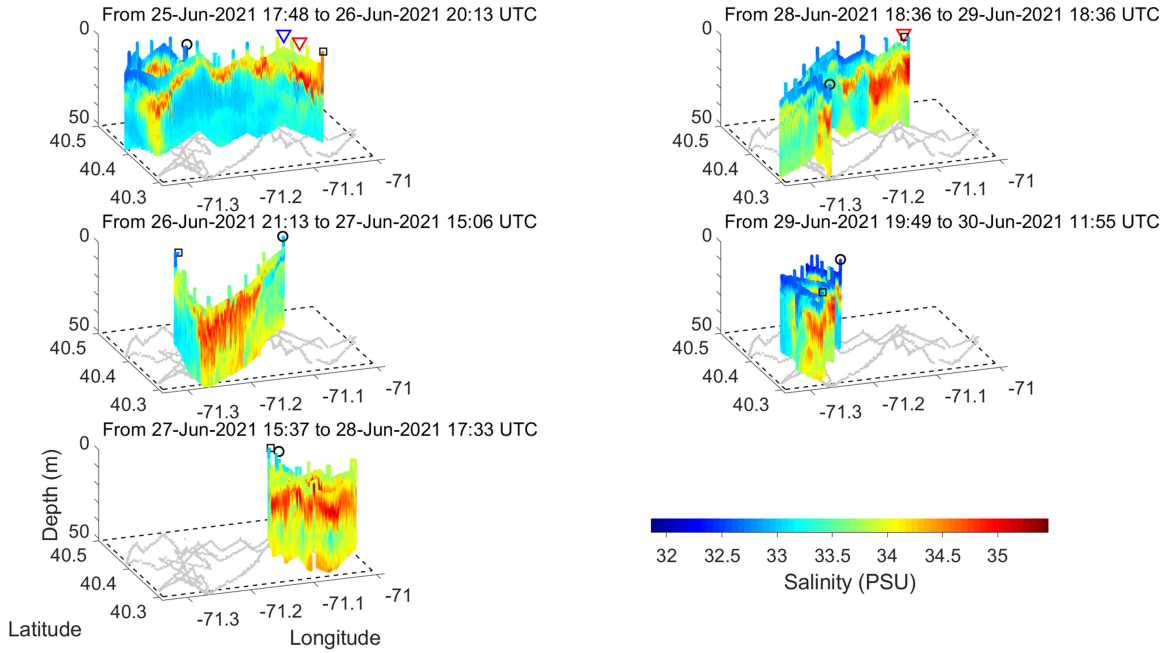

Fig. 8. LRAUV *Polaris* five-day front tracking. The start and the end of each segment is marked by the square and the circle, respectively. The locations and times of the red and blue triangles in the upper-left and upper-right panels are used to estimate the advancement speed of the front (see text). The gray lines show *Polaris*' horizontal-dimension track during the five-day front tracking. The dashed line box marks the bounds.

progress against a westward current. Consequently, when the front was detected, the turn angle from "northeast" to south or from south to "northeast" was 120° (rather than 135°).

5) Continued Flight Distance After Detecting the Front: Every time the LRAUV detected the front, it continued flight for 24 min (equivalent to about 1-km distance). On the zigzag tracks, the 1-km continued flight distance (marked green in Fig. 4) into both sides of the front provided a good depiction of the frontal zone.

6) Front-Tracking Bounds: The LRAUV front-tracking bounds were set to 40.3°N–40.5°N and 71°W–71.333°W, as marked by the dashed line box in Fig. 5. If the LRAUV reached the western/eastern bound, it would switch to the next eastward/westward sweep. If the LRAUV reached the northern

or southern bound without detecting the front (or during the continued flight after detecting the front), it would make a 135° turn onto the next transect back into the bounding box.

C. Cross-Front Transects

On June 25, *Polaris* started on a northward transect on a westward sweep, as shown in Fig. 6. In this mission, *Polaris* detected and crossed the salinity-intrusion front five times. Fig. 7 shows salinity measured on each yo-yo profile and the corresponding ΔS_{vert}. The yo-yo profiles on which ΔS_{vert} met the $\mathrm{thresh}_{\Delta S_{\mathrm{vert}}}$ criterion are marked red. When the count of "red" yo-yo profiles reached 5, *Polaris* determined that it had crossed the front and entered the other water type. After each detection, *Polaris* continued flight for 24 min to survey the frontal zone. In Figs. 6 and 7, *Polaris*' dead-reckoned latitude and longitude are corrected using the periodic GPS fixes. Based on the corrections, there was a westward current of about 0.15 m/s during this LRAUV mission.

D. Front Tracking Over Five Days

Polaris tracked the salinity-intrusion front's movement from June 25 to 30, as shown in Fig. 8. The transects provided high-resolution three-dimensional mapping of the front's structure. We observed the following.

1) The front's orientation was largely east–west (between saltier water to the south and fresher water to the north). The salinity intrusion appeared to be stronger (i.e., higher salinity) to the east.
2) Comparison between June 25–26 and 28–29 (upper-left and upper-right panels in Fig. 8, respectively) showed that the front was advancing northward in this duration. In the upper-left panel, the red triangle marks the location of the high-salinity tongue; the blue triangle marks the location of low salinity. In the upper-right panel, the high-salinity tongue had advanced northward to a location marked by the red triangle (this location was the same as that marked by the blue triangle in the upper-left panel). The latitudinal separation between the red and blue triangles in the upper-left panel was 3.8 km. The time difference between the blue triangle in the upper-left panel and the red triangle in the upper right panel was three days (same location at different times). Thus, the front's northward advancement speed was estimated to be about 1.3 km/day.

These observations combine to indicate that the saltier water was intruding onto the shelf, consistent with the theory [1].

V. Conclusion

We have developed a method for an AUV to autonomously detect, map, and track a salinity-intrusion front. LRAUV *Polaris* tracked a salinity-intrusion front on the southern New England shelf for five days and effectively revealed the spatial structure (along-depth, along-front, and cross-front) and movement of the front. The advancement of autonomous sampling platforms and algorithms allows us to investigate complex spatio-temporal structures, such as salinity intrusions, which has not been possible to this detail before.

The key to developing successful AUV algorithms is combining oceanographic insight with the AUV's flexible behaviors. In our case, oceanographic insight pointed to the vertical structure of salinity as the distinct feature for distinguishing the salinity intrusion from the fresher water. The front-detection problem was thus reduced to calculating a simple metric, the VSHI, and comparing it with a threshold. The AUV's yo-yo behavior suits real-time calculation of VSHI on each yo-yo profile, and the vehicle's readiness to change heading makes zigzag front tracking realizable.

In the presented experiment, the front-tracking algorithm parameters were set based on historical information and LRAUV reconnaissance surveys. To make the algorithm more adaptive to the dynamic environments, we consider improvements in the following aspects.

A. Polygon Bounding Box

To keep the AUV away from operational hazards (shallow bathymetry, ship traffic, high currents, etc.) and within the area of interest, we often need to define a bounding box of a more complex shape than a rectangle. In previously developed upwelling front-tracking algorithms for AUVs or Wave Gliders, the bounding box can be specified to have slanted slides [10] or as a polygon [11]. We need to port these functionalities to the salinity front-tracking algorithm.

B. Adaptive Adjustment of $\mathrm{thresh}_{\Delta S_{\mathrm{vert}}}$

In autonomous classification algorithms, threshold setting is unavoidable. Prior information and *in situ* measurements are used for setting an appropriate $\mathrm{thresh}_{\Delta S_{\mathrm{vert}}}$ to minimize the total cost of misclassification. For *Polaris* missions from June 25 to 27 (column 1, rows 1 and 2 in Fig. 8), we set $\mathrm{thresh}_{\Delta S_{\mathrm{vert}}}$ to 0.4 PSU, which was at the middle of the ΔS_{vert} levels of the two distinct water types. However, in the June 26–27 mission (column 1, row 2 in Fig. 8), it turned out that the threshold was too high such that *Polaris* did not detect the front but reached all the way to the southern bound. Accordingly, we lowered $\mathrm{thresh}_{\Delta S_{\mathrm{vert}}}$ to 0.3 PSU for *Polaris* missions from June 27 to 30 (column 1, row 3 and column 2, rows 1 and 2 in Fig. 8). One approach to autonomous adjustment of $\mathrm{thresh}_{\Delta S_{\mathrm{vert}}}$ is: on every transect across the front, the AUV records ΔS_{vert} levels of the two water types; when one level or both levels change, the algorithm dynamically maintains $\mathrm{thresh}_{\Delta S_{\mathrm{vert}}}$ at the middle level.

C. Adaptive Adjustment of Yo-Yo Depth Range and Participating Depths for Calculating ΔS_{vert}

Based on prior information of the depth and thickness of the salinity intrusions, we set the participating depths for calculating ΔS_{vert} that brings out the contrast between the two distinct water types, and then set the AUV yo-yo depth range to contain all the participating depths. When environmental conditions change, the salinity intrusion's depth and thickness may accordingly

change. By monitoring the changes of the salinity intrusion's vertical profile, the algorithm can autonomously adjust the settings of the participating depths for calculating ΔS_{vert} and the yo-yo depth range. For example, when the salinity intrusion deepens, the algorithm will autonomously deepen some of the participating depths and the lower bound of the yo-yo depth range.

ACKNOWLEDGMENT

The authors would like to thank S. Prasad for assisting with the LRAUV operation, M. Andres for supplying the Gulf Stream path data, and *R/V Neil Armstrong* crew. The AVHRR SST data are available through MARACOOS (http://tds.maracoos.org/thredds/catalog.html), and the SMAP SSS data are available through the NOAA CoastWatch portal (https://coastwatch.noaa.gov/cw/satellite-data-products/sea-surface-salinity/miras-smos.html), both accessed on September 8, 2021. The authors appreciate the helpful comments from the three anonymous reviewers for improving this article.

REFERENCES

[1] G. G. Gawarkiewicz, C. A. Linder, J. F. Lynch, A. E. Newhall, and J. J. Bisagni, "A surface-trapped intrusion of slope water onto the continental shelf in the Mid-Atlantic Bight," *Geophys. Res. Lett.*, vol. 23, no. 25, pp. 3763–3766, 1996.

[2] G. T. Csanady and P. Hamilton, "Circulation of slopewater," *Continental Shelf Res.*, vol. 8, no. 5, pp. 565–624, 1988.

[3] S. J. Lentz, "A climatology of salty intrusions over the continental shelf from Georges Bank to Cape Hatteras," *J. Geophys. Res.*, vol. 108, no. C10, pp. 1–2, 2003.

[4] C. A. Linder and G. Gawarkiewicz, "A climatology of the shelfbreak front in the Middle Atlantic Bight," *J. Geophys. Res.*, vol. 103, no. C9, pp. 18405–18423, 1998.

[5] J. P. Ryan, J. A. Yoder, J. A. B. Barth, and P. C. Cornillon, "Chlorophyll enhancement and mixing associated with meanders of the shelf break front in the Mid-Atlantic Bight," *J. Geophys. Res.*, vol. 104, no. C10, pp. 23479–23493, 1999.

[6] A. Hoarfrost *et al.*, "Gulf Stream ring water intrusion on the Mid-Atlantic Bight continental shelf break affects microbially driven carbon cycling," *Frontiers Mar. Sci.*, vol. 6, 2019, Art. no. 394.

[7] G. Gawarkiewicz *et al.*, "The changing nature of shelf-break exchange revealed by the OOI Pioneer Array," *Oceanography*, vol. 31, no. 1, pp. 60–70, 2018.

[8] M. Andres, "On the recent destabilization of the Gulf Stream path downstream of Cape Hatteras," *Geophys. Res. Lett.*, vol. 43, pp. 9836–9842, 2016.

[9] E. D'Asaro, C. Lee, L. Rainville, R. Harcourt, and L. Thomas, "Enhanced turbulence and energy dissipation at ocean fronts," *Science*, vol. 332, pp. 318–322, 2011.

[10] Y. Zhang, J. G. Bellingham, J. P. Ryan, B. Kieft, and M. J. Stanway, "Autonomous four-dimensional mapping and tracking of a coastal upwelling front by an autonomous underwater vehicle," *J. Field Robot.*, vol. 33, pp. 67–81, 2016.

[11] Y. Zhang *et al.*, "Autonomous tracking of an oceanic thermal front by a wave glider," *J. Field Robot.*, vol. 36, pp. 940–954, 2019.

[12] A. K. Wåhlin *et al.*, "Pathways and modification of warm water flowing beneath Thwaites Ice Shelf, West Antarctica," *Sci. Adv.*, vol. 7, pp. 1–9, 2021.

[13] T. Fossum, P. Norgren, I. Fer, F. Nilsen, Z. C. Koenig, and M. Ludvigsen, "Adaptive sampling of surface fronts in the Arctic using an autonomous underwater vehicle," *IEEE J. Ocean. Eng.*, vol. 46, no. 4, pp. 1155–1164, Oct. 2021.

[14] I. Belkin, J. Borges de Sousa, J. Pinto, R. Mendes, and F. López-Castejón, "A new front-tracking algorithm for marine robots," in *Proc. IEEE/OES Auton. Underwater Veh. Workshop*, Porto, Portugal, 2018, pp. 1–3.

[15] B. Hobson, J. G. Bellingham, B. Kieft, R. McEwen, M. Godin, and Y. Zhang, "Tethys-class long range AUVs—Extending the endurance of propeller-driven cruising AUVs from days to weeks," in *Proc. IEEE/OES Auton. Underwater Veh.*, Southampton, U.K., 2012, pp. 1–8.

[16] J. G. Bellingham *et al.*, "Efficient propulsion for the Tethys long-range autonomous underwater vehicle," in *Proc. IEEE/OES Auton. Underwater Veh.*, Monterey, CA, USA, 2010, pp. 1–6.

[17] J. G. Bellingham and T. R. Consi, "State configured layered control," in *Proc. IARP 1st Workshop Mobile Robots Subsea Environments*, Monterey, CA, USA, 1990, pp. 75–80.

[18] G. Gawarkiewicz, R. K. McCarthy, K. Barton, A. K. Masse, and T. M. Church, "A Gulf Stream-derived pycnocline intrusion on the Middle Atlantic Bight shelf," *J. Geophys. Res.*, vol. 95, no. C12, pp. 22305–22313, 1990.

[19] G. Gawarkiewicz and A. M. Mercer, "Partnering with fishing fleets to monitor ocean conditions," *Annu. Rev. Mar. Sci.*, vol. 11, pp. 391–411, 2019.

[20] K. Fukunaga, *Introduction to Statistical Pattern Recognition*. 2nd ed., Cambridge, MA, USA: Academic, pp. 131–153, 1990.

[21] H. L. Van Trees, *Detection, Estimation, and Modulation Theory, Part I*. New York, NY, USA: Wiley, 1968, pp. 23–46.

[22] A. Branch *et al.*, "Front delineation and tracking with multiple underwater vehicles," *J. Field Robot.*, vol. 36, pp. 568–586, 2019.

[23] Y. Zhang, J. P. Ryan, J. G. Bellingham, J. B. J. Harvey, and R. S. McEwen, "Autonomous detection and sampling of water types and fronts in a coastal upwelling system by an autonomous underwater vehicle," *Limnology Oceanogr.: Methods*, vol. 10, pp. 934–951, 2012.

[24] M. A. Godin, J. G. Bellingham, B. Kieft, and R. McEwen, "Scripting language for state configured layered control of the Tethys long range autonomous underwater vehicle," in *Proc. MTS/IEEE Oceans'10*, Seattle, WA, USA, 2010, pp. 1–7.

Yanwu Zhang (Senior Member, IEEE) was born in Shaanxi, China, in 1969. He received the B.S. degree in electrical engineering and the M.S. degree in underwater acoustics engineering from Northwestern Polytechnic University, Xi'an, China, in 1989 and 1991, respectively, the M.S. degree in electrical engineering and computer science from the Massachusetts Institute of Technology (MIT), Cambridge, MA, USA, in 1998, and the Ph.D. degree in oceanographic engineering from the MIT/Woods Hole Oceanographic Institution Joint Program, Cambridge/Woods Hole, MA, USA, in 2000.

From 2000 to 2004, he was a Systems Engineer working on medical image processing with the General Electric Company Research and Development Center, Niskayuna, NY, USA, and then a Senior Digital Signal Processing Engineer working on digital communications with Aware, Inc., Bedford, MA, USA. Since December 2004, he has been with the Monterey Bay Aquarium Research Institute, Moss Landing, CA, USA, first as a Senior Research Specialist and then as a Senior Research Engineer. He leads the project of targeted sampling by autonomous vehicles, designs adaptive sampling algorithms for marine ecosystem studies, and participated in the development of the *Tethys*-class long-range autonomous underwater vehicles (AUVs). Since 1996, he has participated in more than a dozen field experiments running the *Odyssey* IIB, *Dorado*, and *Tethys* AUVs.

Dr. Zhang was a finalist of the *MIT Technology Review's* 100 young innovators (TR100) as a Ph.D. student in 1999. He was awarded the Visiting Fellowship of Antarctic Gateway Partnership from the University of Tasmania, Hobart, TAS, Australia, in 2018. He was a plenary speaker at the 2020 IEEE OES Autonomous Underwater Vehicle Symposium. He is currently an Associate Editor for *Frontiers in Marine Science* in the specialty section of Ocean Observation. He is a member of Sigma Xi.

Noa Yoder was born in New York City, NY, USA, in 1997. She received the B.S. degree in mechanical and ocean engineering from the Massachusetts Institute of Technology, Cambridge, MA, USA, in 2019.

Since 2019, she has been a Mechanical Engineer with the Woods Hole Oceanographic Institution (WHOI), Woods Hole, MA, USA. Her work focuses on developing autonomous underwater vehicle payloads and capabilities for oceanographic research and environmental response. At WHOI, she also leads operations and field work for both the *Tethys*-class long-range AUVs and the Remote Environmental Monitoring Units (REMUS) AUVs.

Brian Kieft (Member, IEEE) received the B.S. degree in computer science from Hope College, Holland, MI, USA, in 2001.

From 2001 to 2006, he was with the avionics industry, developing and testing subsystems for military aircraft. In 2006, he joined the Monterey Bay Aquarium Research Institute, Moss Landing, CA, USA, as a Software Engineer. He has worked on various platforms, including mooring controllers, benthic instruments, Wave Gliders, and several autonomous underwater vehicles (AUVs) and their associated payloads. He has also been actively involved in updating and teaching the IEEE tutorial "AUV Technology and Application Basics" since 2011. He also cochairs the Wave Glider users' group. His current research interests include development of the *Tethys*-class AUV—a long-range, upper-water-column AUV designed primarily for biological sensing. Apart from development, he also takes part in mission planning and payload integration for ongoing collaborative field programs and engineering tests.

Amy Kukulya received the B.S. degree in environmental policy from Rutgers University, New Brunswick, NJ, USA, in 1999.

Her career in marine robotics spans across a multidisciplined approach with Woods Hole Oceanographic Institution, Woods Hole, MA, USA, specializing in scientific applications of autonomous underwater vehicles (AUVs). She is currently a Research Engineer, and the Director and Principal Investigator of the Scibotics Laboratory in the Applied Ocean Physics and Engineering Department. Working with underwater robots has brought her from the Arctic to Antarctica. She has either led or participated in more than 98 oceanographic expeditions to date. She is currently the Lead Developer of SharkCam as featured on Shark Week. Her work has also been featured on several Discovery Channel and PBS productions as well as the *Boston Globe*, *Washington Post*, and *National Geographic Magazine*. She holds two patents and is currently Co-Principal Investigator on several projects, including leading a Department of Homeland Security Center of Excellence project for underice and oil spill mapping using ocean robots. Her technical interests include configuration and operations of AUV systems, including navigation, imaging capabilities, and new sensor development.

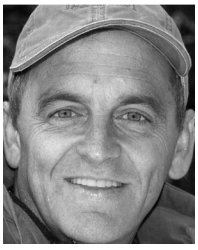

Brett W. Hobson (Member, IEEE) received the B.S. degree in mechanical engineering from San Francisco State University, San Francisco, CA, USA, in 1989.

He began his ocean engineering career with Deep Ocean Engineering, San Leandro, CA, USA, developing remotely operated vehicles. In 1992, he helped start and run Deep Sea Discoveries, where he helped develop and operate deep-towed sonar and camera systems offshore the United States, Venezuela, Spain, and the Philippines. In 1997, he joined Nekton Research, Durham, NC, USA, to develop bioinspired underwater vehicles for Navy applications. After the merging of Nekton Research into iRobot in 2005, he joined the Monterey Bay Aquarium Research Institute, Moss Landing, CA, USA, where he leads the development of the long-range autonomous underwater vehicles. He has been the PI or Co-PI on numerous ONR, NSF, DHS, and NASA projects to develop and operate various subsea vehicles for ocean science.

Svenja Ryan was born in Lörrach, Germany, in 1989. She received the B.S. degree in physics of the Earth system in 2012 and the M.S. degree in climate physics in 2014, both from Kiel University, Kiel, Germany in collaboration with GEOMAR, Helmholtz Centre for Ocean Research Kiel, Germany, and the Ph.D. degree in physical oceanography from the University of Bremen and the Alfred Wegener Institute, Helmholtz Centre for Polar and Marine Research, Bremerhaven, Germany, in 2018.

In 2019, she joined the Woods Hole Oceanographic Institution, Woods Hole, MA, USA, as a postdoc with a Feodor-Lynen fellowship from the Alexander von Humboldt foundation. Her research interests are multifaceted and she has worked with various datasets and in multiple regions. In her Ph.D. research, she studied warm water transport to one of the largest ice shelves in Antarctica based on observational data (moorings and CTDs) as well as modeling. Since her postdoc, she is studying marine heatwaves, in particular their depth structures and associated drivers, using high-resolution global ocean model output. After focusing on the southeast Indian Ocean, she is currently working on the Northeast U.S. continental shelf.

Glen G. Gawarkiewicz received the S.B. degree in ocean engineering from the Massachusetts Institute of Technology, Cambridge, MA, USA, in 1981, and the Ph.D. degree in physical oceanography from the University of Delaware, Newark, DE, USA, in 1989.

He is currently a Senior Scientist with the Physical Oceanography Department, Woods Hole Oceanographic Institution (WHOI), Woods Hole, MA, USA. He was a Postdoctoral Investigator with WHOI and joined the scientific staff in 1991. His research interests include continental shelf and slope dynamics with particular emphasis on shelf-break processes. He has been working with autonomous underwater vehicles since 2004 and has used the vehicles in a variety of scientific applications, including the shelf-break front in the Middle Atlantic Bight, the coastal current east of Cape Cod, and Glovers Reef in Belize. He led the team that provided the conceptual design for the Ocean Observatories Initiative Pioneer Array and he has used this observatory to study how ocean processes are changing as the ocean is warming. He also works extensively with ocean acousticians and with the commercial fishing industry on community science.